PROGRESS IN PHOTOVOLTAICS: RESEARCH AND APPLICATIONS
Prog. Photovolt. Res. Appl. 2007; **15**:493–505
Published online 2 March 2007 in Wiley InterScience (www.interscience.wiley.com) DOI: 10.1002/pip.755

Research

Series Resistance Characterization of Industrial Silicon Solar Cells With Screen-printed Contacts Using Hotmelt Paste

A. Mette*,†, D. Pysch, G. Emanuel, D. Erath, R. Preu and S. W. Glunz
Fraunhofer Institute for Solar Energy Systems, Heidenhofstr. 2, D-79110 Freiburg, Germany

This work presents the results of a detailed series resistance characterization of silicon solar cells with screen-printed front contacts using hotmelt silver paste. Applying the hotmelt technology energy conversion efficiencies up to 18·0% on monocrystalline wafers with a size of 12·5 cm × 12·5 cm have been achieved, an increase of 0·3% absolute compared to cells with conventional screen-printed contacts. This is mainly due to the reduction in the finger resistance to values as low as 14 Ω/m, which reduces the series resistance of the solar cell significantly. To retrieve the lumped series resistance as accurately as possible under the operating condition, different determination methods have been analyzed. Methods under consideration were fitting of the two-diode equation function to a dark IV-curve, integration of the area A under an IV-curve, comparison of a j_{sc}–V_{oc} with a one-sun IV-curve, comparison of the j_{sc} and V_{oc} points of a shaded curve with the one-sun IV-curve as well as comparison of a dark IV-curve with a one-sun IV-curve, and comparison of IV-curves measured at different light intensities. The performed investigations have shown that the latter four methods all resulted in reliable series resistance values. Copyright © 2007 John Wiley & Sons, Ltd.

KEY WORDS: characterization; series resistance; photovoltaic cells; screen-printing

Received 16 November 2006; Revised 15 January 2007

INTRODUCTION

In industrial production the most applied technique for front side metallization of silicon solar cells is still screen-printing, a reliable and well-known process with high throughput rates. Admittedly, the potential of conventional screen-printing is limited, for example in attaining a high aspect (height to width) ratio of the final contact. As presented in this paper, higher aspect ratios can be achieved when using hotmelt paste for the

* Correspondence to: A. Mette, Fraunhofer Institute for Solar Energy Systems, Heidenhofstr. 2, D-79110 Freiburg, Germany.
†E-mail: ansgar.mette@ise.fraunhofer.de

front side metallization due to the temperature difference used in the process and the higher silver content compared to conventional paste. The hotmelt paste is solid at room temperature and can be processed as conventional ink, when melted on a resistively heated screen. A drying step after printing is not necessary as the ink re-solidifies immediately after the printing process. The higher aspect ratio reduces the line resistivity and hence the series resistance significantly; higher energy conversion efficiencies can be achieved.

Concentrating on the front side structure reducing the doping concentration of the emitter would also lead to a higher efficiency potential. But till now contacting high sheet resistance emitters ($R_{sheet} > 80\,\Omega$/sq) in industrial application with thick film technologies result in very high contact resistances limiting the cell performance.[1]

The accurate determination of the series resistance R_S is very important to localize dominant loss mechanisms in the solar cell. Solar cells produce high currents at fairly low voltages; hence already a modest rise in the series resistance can result in a large power loss increase.

Thus, keeping the series resistance as low as possible is certainly of major importance. However, as for example for the front side structure, which is responsible for the dominant contribution to the over-all series resistance, an optimum between losses due to grid shading and electrical losses due to the series resistance have to be found. Therefore both values need to be determined as accurately as possible, for example grid finger width optimization. Whereas the measurement of shading losses is straight forward, the determination of the series resistance depends on the measuring method applied. Results can differ strongly.

For example the series resistance can be measured under illuminated and under non-illuminated conditions. The value determined under illumination is the most interesting one for us as it is measured under real operating conditions. This series resistance is usually higher than the series resistance measured without illumination, due to different current flow pattern in each state.[2,3] Therefore in addition to the hotmelt technology a detailed comparison of different methods to determine the series resistance of these solar cells as accurate as possible is presented.

SCREEN-PRINTED SILICON SOLAR CELLS USING THE HOTMELT TECHNOLOGY

Hotmelt technology

A new type of silver screen-printing paste has been recently introduced by Ferro, USA. This hotmelt paste is solid at room temperature and printable at elevated temperatures of around 50–90°C.[4,5] Hence all the components in contact with the paste have to be heated, which includes the squeegees, the print nest, and the screen. Due to different paste properties, as for example an increased silver content compared to conventional paste, the different printing processes applied, and the different temperatures used during the process, high aspect ratios can be achieved. Figure 1 shows a cross section of a printed and fired contact finger attained, using the hotmelt and the conventional technology. Whereas the finger width of 120 μm is the same, the height of 30 μm for the hotmelt printed contact is significantly increased compared to the conventional printed one with a maximum height of 13 μm. The specific resistivity of $2{\cdot}9$–$3{\cdot}5 \times 10^{-8}\,\Omega\,m$ for the bulk of the hotmelt printed fingers is similar or even less to the one for conventional paste. But due to the higher aspect ratio and hence finger cross section area the resistance per length decreases significantly. Line resistance of about 14 Ω/m has been measured in the dark using a four point probe setup which is equal to a normalized finger resistance, the resistance per finger length times its width, of $1{\cdot}68\,m\Omega$, a very low value for a single screen-printed contact. For the conventional printed contact a finger resistance of 34 Ω/m has been obtained.

The contact resistivity ρ_c, the resistance between the metal and the semiconductor surface, was measured using the transfer length method (TLM).[6,7] For the optimized firing process, contact resistivities as low as 1–3 $m\Omega\,cm^2$ have been achieved to the emitter surface with a sheet resistivity of 40 Ω/sq for both paste types.

DOI: 10.1002/pip

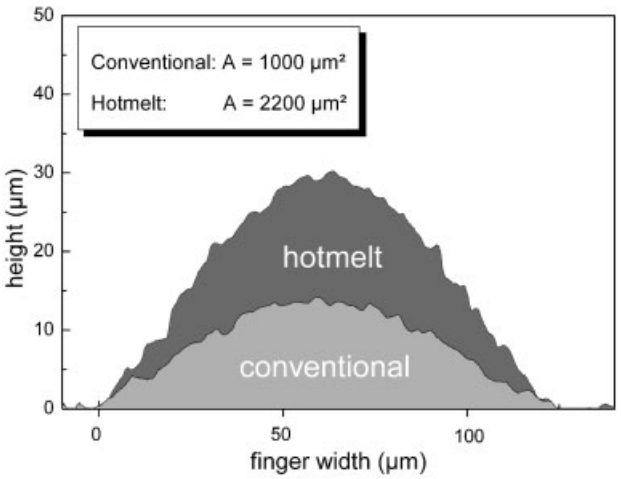

Figure 1. Cross sections of contact fingers achieved by the hotmelt and the conventional technology

IV-parameters of hotmelt versus conventional screen-printed solar cells

At Fraunhofer ISE solar cells were processed on 270 µm thick boron-doped Cz-silicon wafers with a base resistivity of 3–6 Ω cm and a size of 12·5 cm × 12·5 cm. These cells exhibit a textured surface with an emitter sheet resistance of 40 Ω/sq covered by a sputtered SiN_X:H antireflection coating. After conventional aluminum-screen-printing and drying of the rearside, the front-side of one part of the batch was printed with hotmelt, the rest of the batch with conventional paste. A drying step for the hotmelt printed contacts is not necessary. The wafers were co-fired in a fast firing single wafer furnace[8] and then edge-isolated by laser scribing and cleaving.

With this simple industrial-like process, hotmelt screen-printed cells with an energy conversion efficiency up to 18·0% and a fill factor of 80·2% were fabricated (see Table I). The remarkable efficiency of 17·9% averaged over eight cells from the same batch, printed and fired with the same process parameters, points out the very good reproducibility. Also for the conventional printed cells excellent efficiencies up to 17·7% could be achieved. Comparing the mean values, the higher fill factor of about 0·8% absolute for the hotmelt printed contacts compared to the reference cells is mainly attributed to the improved finger conductivity, leading to a lower series resistance of the solar cell. Other parameters as, for example the emitter sheet resistance and the base material affecting the fill factor are very similar for both types of solar cells due to the same cell structure and the same screen used for printing. The efficiency gain for hotmelt screen-printed solar cells is about 0·3% absolute compared to conventional printed cells.

Table I. *IV*-parameter of Cz-Si solar cells with front contacts printed with hotmelt and conventional paste, featuring an emitter sheet resistance of 40 Ω/sq

Cz-silicon	V_{oc} (mV)	j_{sc} (mA/cm^2)	FF (%)	η (%)
Cells printed with hotmelt paste				
Best cell*	624·8	36·0	80·2	18·0
Avg. of 8 cells	621 ± 1	36·0 ± 0·1	80·0 ± 0·3	17·9 ± 0·1
Cells printed with conventional paste				
Best cell	620·7	36·0	79·2	17·7
Avg. of 4 cells	621 ± 1	35·8 ± 0·2	79·2 ± 0·1	17·6 ± 0·1

*Calibrated measurement at Fraunhofer ISE CalLab.

DOI: 10.1002/pip

Table II. *IV*-parameters of 12·5 cm × 12·5 cm Cz-Si solar cells with front contacts printed with hotmelt paste featuring an emitter sheet resistivity of 40 Ω/sq and 55 Ω/sq

Cz-silicon	V_{oc} (mV)	j_{sc} (mA/cm^2)	FF (%)	η (%)
40 Ω/sq emitter sheet resistance				
Best cell	621·0	35·7	80·4	17·8
Avg. of 12 cells	619 ± 1	35·9 ± 0·1	79·4 ± 0·4	17·7 ± 0·1
55 Ω/sq emitter sheet resistance				
Best cell	621·0	36·5	79·5	18·0
Avg. of 12 cells	620 ± 1	36·5 ± 0·2	78·9 ± 0·3	17·9 ± 0·1

These cells followed a complete industrial process.

Comparison of hotmelt printed solar cells with different sheet resistance emitter

In a subsequent batch textured monocrystalline Cz-silicon solar cells of 12·5 cm × 12·5 cm with a sheet resistivity of 40 and 55 Ω/sq were pre-processed opposed to the first batch in an industrial production line including PECVD SiN antireflection coating. At Fraunhofer ISE the rearside was screen-printed with conventional Al paste and dried. The front pattern was screen-printed with Ag hotmelt paste. The wafers were co-fired in a standard inline fast firing belt furnace, opposed to the first batch in which the wafers were fired in a single wafer furnace. Finally, the wafers were edge isolated by laser scribing and cleaving.

High energy conversion efficiencies up to 18·0% for solar cells with a 55 Ω/sq emitter sheet resistance and up to 17·8% for the 40 Ω/sq have been achieved (see Table II). The average efficiency of 17·9% for 12 solar cells processed under the same conditions states the reproducibility of the process on a high level.

Comparing the *IV*-parameters of the solar cells with the two different emitters, the open-circuit voltage nearly remains the same due to the non-optimized passivation quality of the antireflection coating, whereas the remarkable high fill factor of 79·4% drops by about 0·5% absolute to 78·9% for the cells with the lower doped emitter. This is due to the increased contact and emitter sheet resistance, increasing the series resistance of the solar cell by about 0·1 Ω cm^2. However, the short-circuit current increases by 1·7% relative due to the improved internal quantum efficiency in the short wavelength region (Figure 2). This significant increase in j_{sc} surpasses the loss in fill factor and results in an efficiency increase of 1·1% relative. One of the best cells with a 55 Ω/sq emitter sheet resistance achieving a fill factor of 79·4% has been analyzed in detail. The base resistivity of the wafer used for this cell is $\rho_{base} = 1$–$3\ \Omega$ cm, the finger width is about 100 μm, and the finger separation distance 2·2 mm. IR-thermographic analysis[9] have shown that the losses due to the series resistance are distributed homogeneously over the solar cell. The emitter sheet resistance (55 Ω/sq), the contact resistance (4 mΩ cm^2),

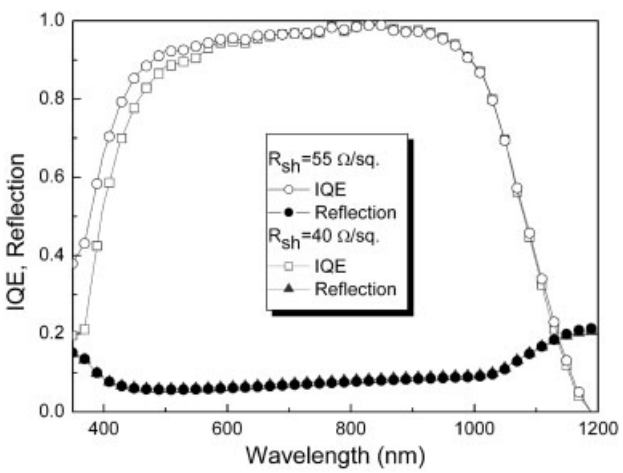

Figure 2. IQE data of a solar cell with a 40 Ω/sq and a 55 Ω/sq emitter sheet resistance

DOI: 10.1002/pip

and the line resistivity of the finger (14 Ω/m), have been measured using the four-point probe technique and the TLM method. With these cell parameters the resistance under illumination for the finger, emitter, base, contact, and busbar could be calculated as for example proposed in Reference [10,11]. For the finger resistance a value $R_{S,finger} = 0{\cdot}10\,\Omega\,cm^2$, for the emitter $R_{S,emitter} = 0{\cdot}20\,\Omega\,cm^2$, for the base $R_{S,base} = 0{\cdot}04\,\Omega\,cm^2$, for the busbar $R_{S,busbar} = 0{\cdot}03\,\Omega\,cm^2$, and for the contact resistance $R_{S,contact} = 0{\cdot}10\,\Omega\,cm^2$ has been determined. Hence for the total ohmic series resistance of one of the best cells a series resistance of $0{\cdot}47\,\Omega\,cm^2$ would be expected.

SERIES RESISTANCE DETERMINATION FROM *IV*-CURVES

The lumped series resistance of a solar cell can be determined directly from *IV*-measurements. In the following six different series resistance determination methods are presented. These methods are furthermore experimentally compared among each other and discussed. The purpose of this investigation is to find a measuring system that is simple, fast and reliable, and can be applied in an industrial environment.

Series resistance determination methods

Fitting of the two-diode equation function to a dark IV-curve

This method is based on an analytical description of a solar cell by the two-diode model:

$$j = j_{01} \cdot \left(\exp\left(\frac{q(V - jR_{S,dark})}{n_1 k_B T} \right) - 1 \right) + j_{02} \cdot \left(\exp\left(\frac{q(V - jR_{S,dark})}{n_2 k_B T} \right) - 1 \right) + \frac{V - jR_{S,dark}}{R_P} - j_{Ph} \qquad (1)$$

j_{01} and j_{02} are the recombination current densities of the emitter/ base and the space charge region, respectively. j_{Ph} is the photo-generated current density, R_P the parallel resistance, k_B the Boltzmann factor, T the temperature, and n_1 and n_2 the ideality factors.

The two-diode equation is fitted to the measured *IV*-points of the dark *IV*-curve. In the upper voltage part the series resistance $R_{S,dark}$ can be extracted, because at this point the power loss due to the series resistance is the most significant loss mechanism.

As stated by Aberle *et al.*[3] the series resistance measured in the dark is lower than the series resistance measured under illuminated conditions due to the different current flow pattern in each state. In dark *IV*-measurements an external current is applied to the electrodes, hence the operating voltage is highest near the electrodes and decreases towards the central emitter region due to the emitter sheet resistance. Under illumination the current flow is reversed, hence the operating voltage is highest in the central emitter region and decreases towards the electrodes.

Comparison of a one-sun with a dark IV-curve

In this method as proposed by Aberle *et al.*[3] the series resistance is determined by comparing the one-sun *IV*-curve at the maximum power point (index mpp) with the dark *IV*-curve shifted by the short-circuit current density j_{sc}:

$$R_{S,light} = \frac{V_{dark,jmpp} - V_{mpp}}{j_{mpp}} \qquad (2)$$

For definition of $V_{dark,jmpp}$ see Figure 3. It is assumed that at small currents the series resistance in the dark *IV*-curve is negligible and the voltage shift between illuminated and dark *IV*-curve is completely due to the illuminated *IV*-curve. Dicker[12] has shown that this method results in a deviation of the series resistance values of at least 5%. Thus, he has introduced an additional term $V_{Rs,dark}$ taking into account the voltage drop due to the series resistance under dark condition $R_{s,dark}$[13]:

$$V_{Rs,dark} = (j_{sc} - j_{mpp}) R_{s,dark} \quad \text{with} \quad R_{S,dark} = \frac{V_{dark,jsc} - V_{oc}}{j_{sc}} \qquad (3)$$

DOI: 10.1002/pip

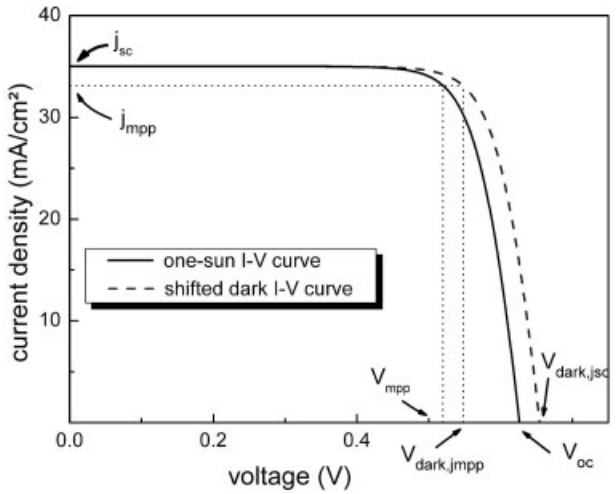

Figure 3. One-sun and by j_{sc} shifted dark *IV*-measurement

The series resistance can finally be determined by:

$$R_{\mathrm{S,light\_dark}} = \frac{\left(V_{\mathrm{dark,jmpp}} - V_{\mathrm{Rs,dark}}\right) - V_{\mathrm{mpp}}}{j_{\mathrm{mpp}}} \tag{4}$$

Comparison of a j_{sc}–V_{oc} with a one-sun IV-curve

The basic assumption for this series resistance determination method is similar to the method described before. A series-resistance-free measurement, the shifted j_{sc}–V_{oc} curve, is compared with the series resistance affected one-sun *IV*-curve at its maximum power point mpp, as illustrated in Figure 4. This was proposed by Wolf in 1963[14] and is described by the following equation:

$$R_{\mathrm{S,Suns}\,V_{\mathrm{oc}}} = \frac{\Delta V}{j_{\mathrm{mpp}}} = \frac{V_{\mathrm{Suns,jmpp}} - V_{\mathrm{mpp}}}{j_{\mathrm{mpp}}} \tag{5}$$

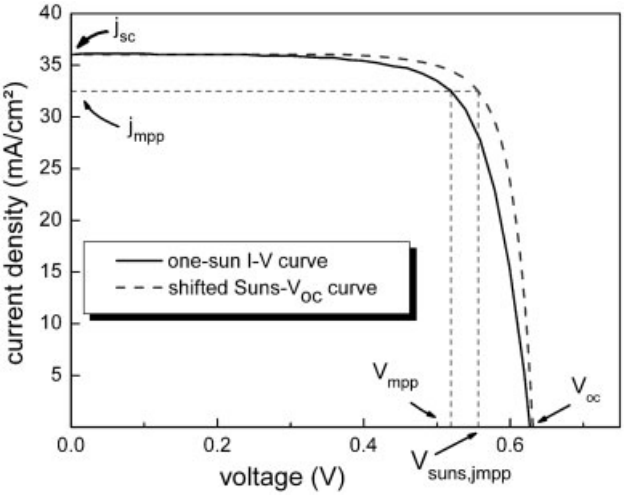

Figure 4. One-sun and shifted j_{sc}–V_{oc} measurement

DOI: 10.1002/pip

$V_{suns,jmpp}$ is equal to the voltage drop of the shifted *Suns*-V_{oc} curve at the maximum power point current density of the one-sun *IV*-curve (see Figure 4). j_{sc} is unaffected from R_S as long as R_S is less than $10\,\Omega\,cm^2$, V_{oc} is unaffected as there is no current flow.[15] Hence the j_{sc}–V_{oc} curve is not influenced by R_S, but it is still affected by j_{02} and R_P.

A simple way of measuring the j_{sc}–V_{oc} curve has been described by Sinton,[16,17] based on the principle of superposition. The open circuit voltage values V_{oc} of a solar cell with known short-circuit current density at one-sun illumination are determined under variation of the light intensity by a flash. The correspondent values of the current density is calculated over a calibrated reference cell. This quick method to determine the j_{sc}–V_{oc} curve of a cell was used in this series resistance determination method.

Comparison of two or more IV-curves measured at different illumination intensities

The comparison of two *IV*-curves at different illumination levels was first proposed by Swanson in 1960.[18] As illustrated in Figure 5, the j_{sc} difference of these curves is due to the linear proportionality of the incident light power to the generated photo current while the V_{oc} shift is due to the smaller voltage drop of the series resistance at a lower light intensity $\Delta V = R_S \Delta j_{sc}$,[14,19] which is exploited in this method.

As proposed in the European Standard EN 60891[20] *IV*-curves at three illumination levels should be measured. On each *IV*-curve a point j_i is chosen in the way that $V_i(j_i)$ is slightly above $V_{i,mpp}$ and that $j_i = j_{sc,i} - \Delta j$. The series resistance R_{S,int_var} can then be determined by calculating the mean value of R_{S1}, R_{S2}, and R_{S3} with:

$$R_{S1} = \frac{V_2 - V_1}{j_1 - j_2} \quad R_{S2} = \frac{V_3 - V_1}{j_1 - j_3} \quad R_{S3} = \frac{V_3 - V_2}{j_2 - j_3} \tag{6}$$

Instead of calculating the mean value, it would be also possible to linearly fit the points (V_i, j_i), the inverted value of the slope is equal to R_{s,int_var}.

As stated by Altermatt *et al.*[15] the assumption for the illumination variation method is, that series resistance, the recombination currents, and the ideality factors are similar at all points (V_i, j_i). This assumption is only justified as long as Δj_{sc} is small. R_s is similar at different illumination levels as long as the sheet resistance of the base is far higher than the sheet resistivity of the emitter and/or $jR_s \leq nkT/q$, otherwise the series resistance declines from a maximum value at the maximum power point to its lowest value at open circuit voltage. Hence to avoid the series resistance dependence at different illumination level Altermatt *et al.* proposed to use the *IV*-curves at 0·9 suns and 1-sun illumination, instead of at 0·5 suns and 1-sun illumination as stated in an earlier article.[14]

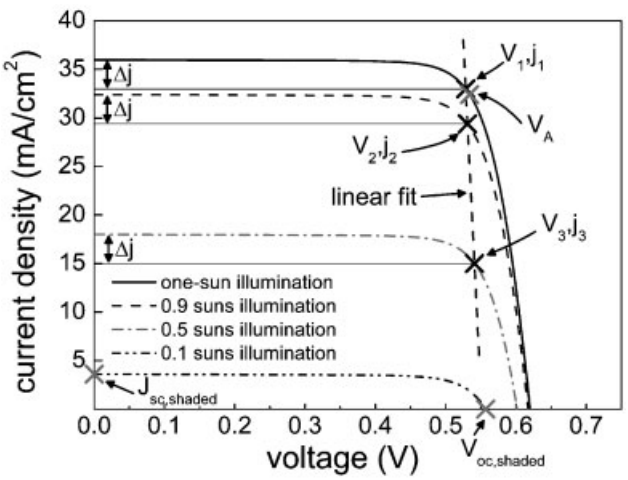

Figure 5. Four *IV*-curves of the same solar cell measured under different illumination intensities

DOI: 10.1002/pip

Comparison of the j_{sc} and V_{oc} values at 0·1 suns illumination intensity with the one-sun IV-curve

This method proposed by Bowden and Rohatgi[21] is based on the illumination intensity variation method and the comparison of the shifted j_{sc}–V_{oc} curve with the one-sun *IV*-curve. The series resistance is determined by comparing the one-sun *IV*-curve with an *IV*-curve shaded to about 0·1 suns illumination intensity; actually just the short circuit current density $j_{sc,shaded}$ and the open circuit voltage $V_{oc,shaded}$ of the shaded curve need to be determined (see Figure 5). Furthermore the voltage point V_A is determined of the one-sun *IV*-curve at the current density $j_{sc} - j_{sc,shaded}$ to achieve the same Δj, as for the shaded curve. The series resistance can then be determined, similar as in the previous described method by:

$$R_{s,shaded} = \frac{V_{oc,shaded} - V_A}{j_{sc} - j_{sc,shaded}} \tag{7}$$

As $V_{oc,shaded}$ is not affected by series resistance, this method is not influenced by the dependence of the series resistance from the illumination level. To determine R_s at the maximum power point the shading level should be chosen in such a way, that $j_{sc} - j_{sc,shaded}$ is equal to j_{mpp}.

Integration of the area under an IV-curve

A very elegant way to determine the series resistance would be to extract the resistance directly from the one-sun *IV*-curve, since just one measurement is necessary. In 1982 a method was suggested by Araujo and Sánchez[22] based on the R_S-modified one diode model equation:

$$j(V) = j_0\left(e^{\frac{(V+jR_S)}{k_B T n_1}} - 1\right) - j_{Ph} \tag{8}$$

This implicit equation in current density is solved for the voltage V and then integrated from zero to short-circuit current density to gain the area A bordered by the one-sun *IV*-curve.

$$A = \int_{j=0}^{j=j_{SC}} V(j)\mathrm{d}j \tag{9}$$

Equation 9 can now be solved for the series resistance and simplified to:

$$R_{S,integral} = 2 \cdot \left(\frac{V_{oc}}{j_{sc}} - \frac{A}{j_{sc}^2} - n_1 \frac{k_B T}{q} \cdot \frac{1}{j_{sc}}\right) \tag{10}$$

As this method is based on the one-diode exponential equation, the series resistance determination will also be affected by a low parallel resistance or a high recombination current. In addition the series resistance is averaged over the whole *IV*-curve, which can underestimate the series resistance at the maximum power point as explained earlier.

Correlation between fill factor and series resistance for industrial silicon solar cells

First a simulation using the two-diode equation function (Eq. 1) was performed to analyze the effect of the series resistance on the fill factor. For the processed cells assumed parameters were $j_{01} = 1{\cdot}3 \times 10^{-12}\,\Omega\,\mathrm{cm}^2$, $j_{02} = 1{\cdot}1 \times 10^{-8}\,\Omega\,\mathrm{cm}^2$, $n_1 = 1$, $n_2 = 2$, and $R_p = 5\,\mathrm{k}\Omega$, whereas the series resistance varied between $R_S = 0\,\Omega\,\mathrm{cm}^2$ and $R_S = 15\,\Omega\,\mathrm{cm}^2$. The fill factor has been extracted and plotted against the series resistance for photo-generation current densities of 32 mA/cm^2, 36 mA/cm^2, and 40 mA/cm^2 as illustrated in Figure 6. The fill factor declines more rapidly for solar cells with higher current densities due to the higher voltage drop caused by the series resistance, whereas FF_0, the fill factor at $R_S = 0\,\Omega\,\mathrm{cm}^2$, almost remains the same. For typical industrial silicon solar cells with a maximum series resistance of $R_S = 2{\cdot}0\,\Omega\,\mathrm{cm}^2$ the data points for each curve can be fitted linearly as also illustrated in Figure 6. For the linear fit with a photo-generation current density of 36 mA/cm^2 the slope m is equal to $5{\cdot}12 \pm 0{\cdot}01\%/\Omega\,\mathrm{cm}^2$ and the $FF_0 = 82{\cdot}17 \pm 0{\cdot}01\%$.

DOI: 10.1002/pip

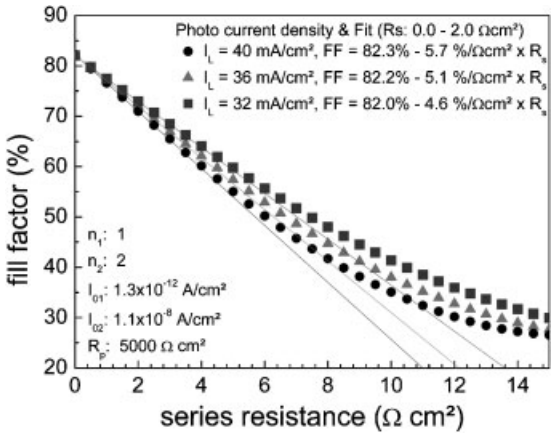

Figure 6. Calculated fill factor plotted against the series resistance for different photo-generation current densities. Data extracted from the two-diode equation function and linear fitted between $R_S = 0\,\Omega\,\mathrm{cm}^2$ and $R_S = 2{\cdot}0\,\Omega\,\mathrm{cm}^2$

The slope of the linear fit can also be calculated directly from the *IV*-parameters with the assumption that j_{sc}, V_{oc}, and j_{mpp} for all the solar cells are constant. An additional series resistance will cause an additional voltage drop ΔV at j_{mpp}.

$$\Delta R_S = \frac{(V_{mpp} + \Delta V_{@j_{mpp}})}{j_{mpp}} - \frac{V_{mpp}}{j_{mpp}} = \frac{\Delta V_{@j_{mpp}}}{j_{mpp}} \tag{11}$$

This assumption is justified since a change of R_S mainly implies a voltage drop and not a change in current.[23] Therefore it should be possible to calculate the slope m_{calc} of the linear fit, by applying the latter assumptions in the definition for the FF and calculating a FF-difference.

$$m_{calc} = \frac{\Delta FF}{\Delta R_S} = \frac{FF_2 - FF_1}{\Delta R_s} = \frac{j_{mpp}(V_1 + \Delta V_{@j_{mpp}}) - j_{mpp}V_1}{\Delta R_s V_{oc} j_{sc}} = \frac{j_{mpp} \cdot \Delta V}{V_{oc} j_{sc} \Delta R_S} = \frac{j_{mpp}^2}{V_{oc} j_{sc}} \tag{12}$$

Hence the expected series resistance for each fill factor point can be approximated by:

$$R_{S,expected} \approx \frac{FF_0 - FF_{measured}}{m} \tag{13}$$

Experimental comparison of the series resistance determination methods

For the experimental comparison 20 solar cells from the batch with the cells, featuring a 55 Ω/sq emitter sheet resistance, were used (compare Section 2·2). As an extensive firing variation has been performed, the fill factor ranged from 73% to 80% due to the differences in the series resistance. All the 20 cells used for the further investigation had a parallel resistance above 3 kΩ cm^2. In order to retrieve the series resistance for each solar cell and determination method, *IV*-curves of the processed cells at three different illumination levels (1 sun, 0·9 suns, and 0·5 suns) were measured using appropriate filters to reduce the irradiance. Additionally, the dark *IV*- and the *Suns*-V_{oc} curve have been measured. The pseudo fill factor (PFF) of the series resistance free *Suns*-V_{oc} *IV*-curve has been extracted for each cell. The mean PFF for all cells is equal to $PFF = 82{\cdot}2 \pm 0{\cdot}2\%$.

The determined series resistance values for each method were plotted against the fill factor and linearly fitted as presented in Figure 7. From these fits the slope m_{fit} and the FF-axis intersection point $FF_{0,fit}$ for each R_S determination method was extracted (see Table III).

Furthermore the fill factor versus series resistance slope was calculated for each solar cell as described in the previous section. This can be done as the values for j_{mpp} ($34{\cdot}0 \pm 0{\cdot}3$ mA/cm^2), V_{oc} (619 ± 2 mV), and j_{sc} ($36{\cdot}3 \pm 0{\cdot}2$ mA/cm^2) can be assumed constant for all the solar cells with an $R_p > 3$ kΩ cm^2 and a fill factor

DOI: 10.1002/pip

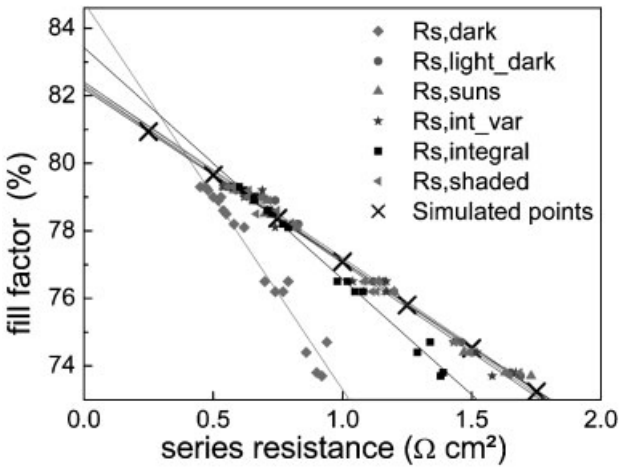

Figure 7. Fill factor of the processed solar cells plotted against the six series resistance determination methods. Data points of each method were fitted linearly

Table III. Experimentally determined values for each R_S method of the fit of the FF versus R_S plot and the correspondent intersection point with the FF-axis in comparison to the theoretical obtained values

R_S method	Slope m (%/Ω cm^2)	FF_0 (%)
Pseudo fill factor	—	82·2 ± 0·2
Calculated value (Eq. 12)	−5·1 ± 0·1	—
Experimentally determined values:		
$R_{S,light\_dark}$	−5·2 ± 0·1	82·4 ± 0·1
$R_{S,Suns}$	−5·1 ± 0·1	82·3 ± 0·1
$R_{S,shaded}$	−5·3 ± 0·1	82·4 ± 0·1
R_{S,int_var}	−5·3 ± 0·2	82·3 ± 0·2
$R_{S,integral}$	−6·9 ± 0·1	83·4 ± 0·1
$R_{S,dark}$	−11·5 ± 0·5	84·8 ± 0·4

above 72%. Using Equation 12 this results in a mean value and standard deviation for the calculated value of $m_{calc} = 5{\cdot}1\%/\Omega\,cm^2 \pm 0{\cdot}1\,\%/\Omega\,cm^2$. This calculated value is very close to simulated value in Section 3·3.

At this point the mean values of m_{calc} and PFF can be compared with each m_{fit} and $FF_{0,fit}$ from the linear fit equations. From this analysis the comparison of the j_{sc} and V_{oc} values of a shaded *IV*-curve with the one-sun *IV*-curve, the comparison of the dark and illuminated *IV*-curve, the comparison of the j_{sc}–V_{oc} and illuminated *IV*-curve and the light intensity variation method seems to be equally good. All the four methods are within the uncertainty range of the theoretical calculated value (see Figure 8 and Table III).

The difference of the series resistance determined from the dark *IV*-curve fit to the expected value is as expected from theory[3] too low, due to the different current flow pattern under illuminated and dark condition. Especially for large area screen-printed silicon solar cells this effect is even increased. On one hand the voltage drop across the typically 30 mm long fingers of a 12·5 × 12·5 cm^2 sized solar cell is not negligible, on the other hand the contact area of about 4·8% under illuminated condition (the current is collected mainly by the fingers) is significantly smaller than the contact area of about 8% (inclusive the 2 mm wide busbars) under dark condition.

The integration method seems to result in fairly good values between 0·5 Ω cm^2 and 0·8 Ω cm^2, but underestimates the series resistance for fill factors below 78%. This could be, because a constant series resistance is assumed over the whole *IV*-curve. When applying the former boundary equation $jR_s \leq nkT/q$ with $j = 34$ mA/cm^2, the series resistance can be expected to be constant just up to a value of about 0·76 Ω cm^2. If all the nine data points between 0·5 Ω cm^2 and 0·76 Ω cm^2 are linearly fitted, this results in fit values of

DOI: 10.1002/pip

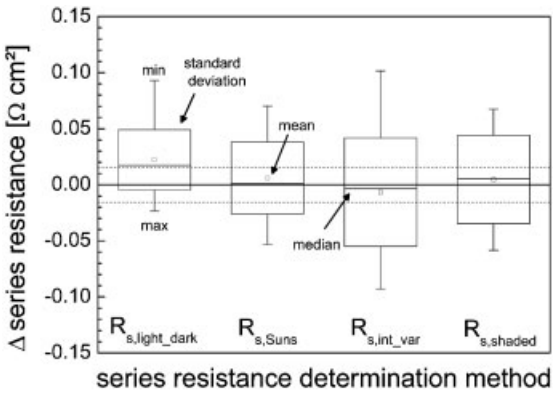

Figure 8. Graph showing the mean, median, minimum, maximum value, and standard deviation for each of the four best series resistance determination methods compared to the expected value (solid line). The expected series resistance value was calculated using Equation 13 including the uncertainty value (dashed line)

$m_{\text{fit}} = -5{\cdot}5\ \%/\Omega\,\text{cm}^2$ and $\text{FF}_{0,\text{fit}} = 82{\cdot}5\%$, a significant improvement compared to the fit parameters over the whole measuring range (compare Table III). Nevertheless, as this method is based on the modified one-diode model equation, and therefore strongly influenced by low parallel resistance and high junction and edge recombination currents, this method is not recommended for series resistance determination.

Although the other four methods seem to be accurate, they need to be carefully applied. A very good agreement with the theoretical values is achieved by comparing the series resistance free j_{sc}–V_{oc} curve with the one-sun *IV*-curve. The fitted slope is very close to the calculated one and also the standard deviation is very small. Nevertheless, when measuring the j_{sc}–V_{oc} curve as proposed by Sinton *et al.*[16] it is important that the base resistivity, the thickness of the cell, the temperature while measuring, as well as the short circuit current density at one-sun illumination is exactly known. In addition, as two different measurement setups are used, there could be a mismatch between the light spectra of the flash and the light source of the sun simulator. The great advantage beside the good series resistance results using this measurement method is that from the *Suns*-V_{oc} measurement additional cell data as for example the PFF can be determined.

The illumination intensity variation values as presented in Table III and Figure 7 was achieved by linearly fitting the V_i, j_i data points of the 1-sun, the 0·9 suns, and the 0·5 suns *IV*-curves. Hereby a small error is introduced as the series resistance for different illumination levels might be different for high R_{s} values. Due to the good agreement with the theoretical values the introduced error seems to be negligible. Whereas, when only using the *IV*-curves at 1 sun and 0·9 suns illumination, the voltage difference at point V_1, j_1 and V_2, j_2 for a solar cell with a series resistance of about $0{\cdot}6\,\Omega\,\text{cm}^2$ is only 2 mV. It is obvious that an accurate *IV*-measurement is crucial, which itself depends on the illumination fluctuation of the sun tester, the number of data points measured around V_i, j_i, the quality of the interpolation function to determine the correct intersection point, and the accuracy of the used measuring systems. Since the 'perfect' measuring condition as proposed in Reference 15 are difficult to achieve in an industrial environment, using the V_i, j_i points of the 1-sun, 0·9 suns, and 0·5 suns is more reliable under practical aspects, even so the values for high series resistance might be slightly underestimated. The advantage of the illumination intensity variation measurement is that the solar cell is measured with the same light source (same spectral response) and the same contacting setup.

Comparing the j_{sc} and V_{oc} values of a 0·1 suns illuminated with the one-sun *IV*-curve also results in series resistance values in good agreement with the theoretical obtained ones. This method combines the advantages of the latter two measuring methods discussed; the same measuring setup and light source can be used and this method is independent on R_{s} variation at different illumination intensities as long as j_{mpp} of the one-sun *IV*-curve is about $j_{\text{sc}} - j_{\text{sc,shaded}}$. In addition, this method is very simple to integrate as just the j_{sc} and V_{oc} values of the shaded *IV*-curve need to be determined.

The comparison of the dark and illuminated *IV*-curve as modified by Dicker results in very reliable series resistance values compared to the calculated ones. A further advantage of this method is that the same contacting

DOI: 10.1002/pip

setup can be used. By measuring the dark *IV*-curve, additional information as, for example the recombination currents and the parallel resistance can be directly extracted.

CONCLUSION

Efficiencies up to 18·0% have been achieved on 12·5 cm × 12·5 cm Cz-silicon solar cells with hotmelt screen-printed front contacts and an aluminum back-surface-field that were completely processed at Fraunhofer ISE as well as on industrial pre-processed cells. The advantage of the hotmelt compared to the conventional technology as well as a reduction of the doping level of the emitter sheet resistance has been demonstrated. Very low line resistivities of 14 Ω/m have been achieved for single screen-printed silver contacts.

Furthermore different series resistance determination methods have been reviewed and experimentally compared. The series resistance of processed solar cells has been extracted with each method. A calculated value for the fill factor drop per series resistance has been compared with the value retained by the slope of the linear fit of the fill factor against series resistance plot for each determination method. In addition the intersection point of the linear fit with the fill factor-axis has been compared with the PFF measured by *Suns-Voc*.

These investigations have shown that in the light intensity variation method, the comparison of the dark with the one-sun *IV*-curve, the comparison of the j_{sc}, V_{oc} points of a shaded curve with the one-sun *IV*-curve, and the comparison of the j_{sc}–V_{oc} curve with the one-sun *IV*-curve are the most accurate methods in order to determine the behavior under operating conditions. To distinguish if one of these four methods is the most accurate one, a higher statistic would be necessary. The fit of the dark *IV*-curve and the integration method results in too low series resistance values.

A detailed series resistance analysis as presented in this work is important for quality assurance and to further improve the performance of industrial silicon solar cells.

Acknowledgements

The authors would like to thank all SOLPRO partners for the successful co-operation and their financial support, G. Wahl, now with Solar Watt Cells GmbH, for supplying the industrial pre-processed solar cells and Ferro GmbH for the hotmelt paste as well as A. Leimenstoll, E. Schäffer, T. Roth, M. Hermle for cell processing, characterization and measurement instruction, and A. Cuevas for fruitful discussion. This work has been supported by the German Federal Ministry for the Environment, Nature Conservation and Nuclear Safety (BMU) under contract no. 329868C and no. 0329960.

REFERENCES

1. Schubert G. *Thick film metallisation of crystalline silicon solar cells. Phd Thesis*, University of Konstanz, Germany, 2006.
2. Nielsen LD. Distributed series resistance effects in solar cells. *IEEE Transactions on Electron Devices* 1982; **29**: 821–827.
3. Aberle AG, Wenham SR, Green MA. *A new method for accurate measurements of the lumped series resistance of solar cells*, *Conference Recordings of 23rd IEEE Photovoltaic Specialists Conference*, Louisville, KY, IEEE, New York, USA, 1993; 133–136.
4. Williams T, McVicker K, Shaikh A, Koval T, Shea S, Kinsey B, Hetzer D. *Hot melt ink technology for crystalline silicon solar cells*, *Conference Recordings of the 29th IEEE Photovoltaics Specialists Conference*, New Orleans, IEEE, New York, USA, 2002; 352–355.
5. Mette A, Erath D, Ruiz R, Emanuel G, Kasper E, Preu R. *Hot melk ink for the front side metallisation of silicon solar cells*, *Proceedings of the 20th European Photovoltaic Solar Energy Conference*, Barcelona, Spain, WIP, Munich, Germany, 2005; 873–876.
6. Murrmann H, Widmann D. Currnet crowding on metal contacts to planar devices. *IEEE Transactions on Electron Devices* 1969; **16**: 1022–1024.

DOI: 10.1002/pip

7. Berger HH. Contact resistance and contact resistivity. *Journal of the Electrochemical Society* 1972; **119**: 507–514.
8. Huljic DM, Biro D, Preu R, Castillo CC, Lüdemann R. *Rapid thermal firing of screen printed contacts for large area crystalline silicon solar cells*, *Proceedings of the 28th IEEE Photovoltaics Specialists Conference*, Anchorage, Alaska, USA, 2000; 379–382.
9. Isenberg J, Warta W. Realistic evaluation of power losses in solar cells by using thermographic methods. *Journal of Applied Physics* 2004; **95**: 5200–5209.
10. Green MA. *Solar cells-operating principles, technology and system applications*, *University of New South Wales*, Australia, 1986.
11. Burgers AR. *New Metallisation Patterns and Analysis of Light Trapping for Silicon Solar Cells*, *Phd Thesis*, University Utrecht, 2005.
12. Dicker J. *Analyse und Simulation von hocheffizienten Silizium-Solarzellenstrukturen für industrielle Fertigungstechniken*, *Phd Thesis*, University of Konstanz, 2003.
13. Rohatgi A, Davis JR, Hopkins RH, Rai-Choudhury P, McMullin PG, McCormick JR. Effect of titanium, copper and iron on silicon solar cells. *Solid State Electronics* 1980; **23**: 415–422.
14. Wolf M, Rauschenbach H. Series resistance effects on solar cell measurements. *Advanced Energy Conversion* 1963; **3**: 455–479.
15. Altermatt PP, Heiser G, Aberle A, Wang A, Zhao J, Robinson SJ, Bowden S, Green M. Spatially resolved analysis and minimization of resistive losses in high-efficiency si solar cells. *Progress in Photovoltaics* 1996; **4**: 399–414.
16. Sinton RA, Cuevas A. A quasi-steady-state open-circuit voltage method for solar cell characterization. *Proceedings of the 16th European Photovoltaic Solar Energy Conference*, Glasgow, 2000; 1152–1155.
17. Sinton RA. *9th Workshop on Crystalline Silicon Solar Cells and Materials*, NREL/BK-520-26941, 1999.
18. Swanson LD. *Private communication with M. Wolf and H. Rauschenbach (see 14).*
19. Handy RJ. Theoretical analysis of the series resistance of a solar cell. *Solid-State Electron.* 1967; **10**: 765–775.
20. European Standard EN60891. Procedures for temperature and irradiances corrections to measured I-V characteristics of crystalline silicon photovoltaic devices, *IEC 891:1987+ A1:1992*, 1994.
21. Bowden S, Rohatgi A. Rapid and accurate determination of series resistance and fill factor losses in industrial silicon solar cells. *Proceedings Of The 17th European Photovoltaic Solar Energy Conference, Munich*, 2001; 1802–1806.
22. Araújo GL, Sánchez E. A new method for experimental determination of the series resistance of a solar cell. *IEEE Transactions on Electron Devices* 1982; **29**: 1511–1513.
23. Swanson RM, Sinton RA. High-efficiency silicon solar cells (chapter 4). In *Advances in Solar Energy (Vol. 6)*, Boer KB, Swanson RM, Sinton RA (eds). Plenum Press: New York, USA, 1990.

DOI: 10.1002/pip